Ship waves in a stratified ocean

By ALBERT A. HUDIMAC

U.S. Navy Electronics Laboratory, San Diego 52, California

(Received 5 July 1960 and in revised form 20 March 1961)

The velocity potential for a simple source moving in a straight line at constant depth in a two-layer ocean is obtained by the Fourier transform method. It is used to develop a formula for the wave-making resistance of a 'thin' ship for both surface and internal waves. An asymptotic expansion is used to delineate quantitatively the internal wave system. It is shown that at speeds less than the critical speed transverse and divergent wave systems are excited, while at speeds greater than the critical internal wave speed only the divergent wave system is excited. Examples of the shape of wave crests and of wave heights are given.

1. Introduction

Free waves in a homogeneous fluid with a free surface are characterized by a maximum vertical displacement at the surface. In deep water, the vertical displacement of a water particle decreases exponentially downward. In stratified water, other types of free waves may occur which are called 'boundary waves' or 'internal waves'. They are characterized by having their greatest vertical displacement in the interior.

The ocean has a vertical density structure. There often is a surface layer (usually quite homogeneous) which is separated from the denser fluid below by a more or less narrow thermocline region. Such layers may be caused by heating, cooling, mixing, and the advection of water masses.

The excitation of waves on the surface of the ocean by a displacement ship has been treated by various approximations. A comprehensive survey is given by Lunde (1951). In practically all cases the ocean is treated as if it were homogeneous; there is very little early literature (see Lamb 1916) on the excitation of internal waves. There has been work on the comparable situation in the stratified atmosphere, e.g. the work of Kochin (1949) and Warren (1960). Ekman (1904) has shown experimentally that a ship moving near the critical internal wave velocity (velocity of waves for which the wavelength is large compared to the thickness of the layer) strongly excites internal waves if the keel depth is about equal to the thickness of the layer. The transfer of energy from the ship to the internal waves is manifested by an increase in resistance to the motion of the ship. Under suitable circumstances, this increase of resistance can be manifold. The phenomenon is referred to as 'dead water'.

The author (1958) developed a formula for the resistance of a 'thin ship' in a two-layer ocean. An algebraic error invalidated the results. One purpose

of this paper is to present the correct results. Sretenskii† (1959) used a somewhat different method of analysis to derive such a formula. It can be shown that the results are exactly equivalent.

Another aspect of ship-excited waves is their peculiar pattern. For a homogeneous ocean, an explanation and treatment of this effect was first given by Kelvin (1887); it has also been treated by many others, e.g. Hogner (1923) and Peters (1949). The pattern of the corresponding internal waves formed in a two-layer ocean is delineated in this paper.

2. Motion of a simple source at constant speed, direction, and depth in a two-layer ocean

For simplicity, a two-layer model of the ocean will be considered. Perturbation theory (see Lunde 1951) can be used to replace a 'thin ship', to the first approximation, by a distribution of simple sources over the centre-plane section. The velocity potential for a simple source in a homogeneous fluid with a free surface has been determined in several ways; it is occasionally called a Havelock source. The objective of this section is to find the corresponding Green's function for a two-layer ocean. The mathematical statement of the problem is given in the next few paragraphs.

Fix a co-ordinate system in space such that the (x, z)-plane lies in the undisturbed interface between a layer of fluid of density ρ, and thickness h, lying on another fluid of density $\rho' = \Delta\rho + \rho$, of semi-infinite extent. Consider a simple point-source moving with constant velocity, c, in the direction of increasing x at a constant distance, f, above the undisturbed interface. If the layer were of infinite extent, the potential would be

$$\phi = m/r_1, \quad r_1^2 = (x-ct)^2 + (y-f)^2 + z^2, \tag{1}$$

assuming the source of strength m to pass over the origin at $t = 0$.

If the source is assumed to have started at $x = -\infty$, then at any finite distance from the origin, the potential ϕ, in the layer, the potential ϕ', below the layer, the pressure, p, the displacement of the free surface, η_s, and the displacement of the interface, η_i, are of the form

$$\left.\begin{aligned} &\phi = \phi(x-ct, y, z), \quad p = p(x-ct, y, z), \quad \eta_s = \eta_s(x-ct, y, z), \\ &\phi' = \phi(x-ct, y, z), \quad \eta_i = \eta_i(x-ct, y, z). \end{aligned}\right\} \tag{2}$$

Now consider a co-ordinate system moving with the source such that the axes $(\bar{x}, \bar{y}, \bar{z})$ are parallel to the stationary axes. Let

$$\bar{x} = x - ct, \quad \bar{y} = y, \quad \bar{z} = z, \quad \bar{t} = t. \tag{3}$$

In the fixed co-ordinate system, the potentials ϕ and ϕ' satisfy Laplace's equation, the former everywhere in the layer except at the source, and the latter everywhere in the lower fluid. The potentials $\overline{\phi}$ and $\overline{\phi}'$ in the moving co-ordinate system still satisfy Laplace's equation, i.e.

$$\Delta\overline{\phi}_b = 0, \quad \overline{\phi} = \overline{\phi}_b + \frac{m}{\bar{r}_1}, \tag{4}$$

† The author is indebted to the referee for having Sretenskii's work brought to his attention.

where the second equation defines $\overline{\phi}_b$, which is assumed to be regular, and

$$\Delta\overline{\phi}' = 0. \tag{5}$$

The boundary conditions can be linearized by a perturbation method. They become, in the moving co-ordinate system,

$$\overline{\phi}_{\bar{y}}(\bar{x}, h, \bar{z}) + c^2 g^{-1}\overline{\phi}_{\bar{x}\bar{x}}(\bar{x}, h, \bar{z}) = 0, \tag{6}$$

$$\rho c^2\overline{\phi}_{\bar{x}\bar{x}}(\bar{x}, 0, \bar{z}) + \rho g\overline{\phi}_{\bar{y}}(\bar{x}, 0, \bar{z}) = \rho' c^2\overline{\phi}'_{\bar{x}\bar{x}}(\bar{x}, 0, \bar{z}) + \rho' g\overline{\phi}'_{\bar{y}}(\bar{x}, 0, \bar{z}), \tag{7}$$

$$\overline{\phi}_{\bar{y}}(\bar{x}, 0, \bar{z}) = \overline{\phi}'_{\bar{y}}(\bar{x}, 0, \bar{z}) = -c\eta_x, \tag{8}$$

where (6) is the combination of the kinematic and dynamic conditions at the free surface (and g is the acceleration of gravity), (7) is the dynamic condition at the interface, and (8) is the kinematic condition at the interface. Also, $\overline{\phi}'$ satisfies the condition

$$\lim_{\bar{y}\to-\infty} \overline{\phi}' = 0, \tag{9}$$

and the condition at infinity has the form

$$\lim_{\bar{x}\to\infty} \overline{\eta}_s = \lim_{\bar{x}\to\infty} \overline{\eta}_i = 0. \tag{10}$$

There is no restriction placed on the η's for $\bar{x} \to -\infty$ except that they be bounded. In sequel, only the moving reference-frame is used and so the bars will be dropped.

The solution of the problem is obtained by application of the Fourier transform method.† The Fourier transform of ϕ_b is

$$\tilde{\phi}_b(\xi, \zeta) = \frac{1}{2\pi}\int\int_{-\infty}^{\infty} \phi_b(x, y, z)\exp\{-i(\xi x + \zeta z)\}\,dx\,dz, \tag{11}$$

and the inverse transform is

$$\phi_b(x, z) = \frac{1}{2\pi}\int\int_{-\infty}^{\infty} \tilde{\phi}_b(\xi, \zeta)\exp\{i(\xi x + \zeta z)\}\,d\xi\,d\zeta.$$

The transform of (4) is

$$\tilde{\phi}_{byy} - (\xi^2 + \zeta^2)\,\tilde{\phi}_b = 0.$$

Let $\xi^2 + \zeta^2 = \varpi^2$. This has the fundamental solution

$$\tilde{\phi}_b = A(\xi, \zeta)\,e^{y\varpi} + B(\xi, \zeta)\,e^{-y\varpi}. \tag{12}$$

Similarly

$$\tilde{\phi}' = A'(\xi, \zeta)\,e^{y\varpi} + B'(\xi, \zeta)\,e^{-y\varpi}. \tag{13}$$

Because of condition (9), $B' = 0$.

The Fourier transform of the surface boundary condition (6) is

$$g\tilde{\phi}_{by}(\xi, h, \zeta) - c^2\xi^2\tilde{\phi}_b(\xi, h, \zeta) - mg\exp\{-\varpi(h-f)\} - \frac{mc^2}{\varpi}\xi^2\exp\{-\varpi(h-f)\} = 0. \tag{14}$$

Here use is made of the well-known relation

$$\frac{1}{(x^2 + (y-f)^2 + z^2)^{\frac{1}{2}}} = \frac{1}{2\pi}\int\int_{-\infty}^{+\infty} \frac{\exp\{\pm\varpi(y-f)\}}{\varpi}\exp\{i(\xi x + \zeta z)\}\,d\xi\,d\zeta, \tag{15}$$

† The method is similar to that used by Timman & Vossers (1953).

where '$-$' is used for $y > f$ and '$+$' is used for $y < f$. Thus the transform of

$$(x^2+(y-f)^2+z^2)^{-\frac{1}{2}}$$

is
$$\mathscr{F}(\exp-[x^2+(y-f)^2+z^2]) = \varpi^{-1}\exp\{\pm\varpi(y-f)\}. \tag{16}$$

The Fourier transforms of the boundary conditions (7) and (8) are

$$\bar{\phi}_{by}(\xi,0,\zeta)+me^{-\varpi f} = \bar{\phi}'_y(\xi,0,\zeta), \tag{17}$$

$$-\rho c^2\xi^2\bar{\phi}_b(\xi,0,\zeta)+\rho g\bar{\phi}_{by}(\xi,0,\zeta)-\rho c^2\varpi^{-1}\xi^2me^{-\varpi f}+\rho gme^{-\varpi f}$$
$$= -\rho' c^2\xi^2\bar{\phi}'(\xi,0,\zeta)+\rho' g\bar{\phi}'_y(\xi,0,\zeta). \tag{18}$$

Substitution of (12) and (13) into (14), (17), and (18) gives a set of three simultaneous equations in A, B, and A'. Solutions are obtained and substituted in (12) and (13) to give $\bar{\phi}_b$ and $\bar{\phi}'$. The inverse transform of $\bar{\phi}_b$ and $\bar{\phi}'$ then gives the formal solutions, ϕ_0 and ϕ'_0, which are not the complete expressions for ϕ and ϕ',

$$\phi_0 = \frac{m}{r_1}+\frac{m}{2\pi}\int\int_{-\infty}^{\infty}\frac{P\exp\{i(\xi x+\zeta z)\}}{Q}\,d\xi\,d\zeta, \tag{19}$$

$$\phi'_0 = \frac{\rho m}{2\pi}\int\int_{-\infty}^{\infty}\frac{2c^2\xi^2Re^{y\varpi}\exp\{i(\xi x+\zeta z)\}}{Q}\,d\xi\,d\zeta, \tag{20}$$

where

$$P = (c^2\xi^2+g\varpi)[-(\rho'+\rho)c^2\xi^2+(\rho'-\rho)g\varpi]\exp\{-(h-f-y)\varpi\}$$
$$-(c^2\xi^2+g\varpi)(c^2\xi^2-g\varpi)(\rho'-\rho)[\exp\{-(h+f-y)\varpi\}+\exp\{-(h-f+y)\varpi\}]$$
$$+(c^2\xi^2-g\varpi)^2(\rho'-\rho)\exp\{(h-f-y)\varpi\},$$
$$Q = \varpi(c^2\xi^2-g\varpi)\{[(\rho'+\rho)c^2\xi^2-(\rho'-\rho)g\varpi]e^{h\varpi}+(c^2\xi^2+g\varpi)(\rho'-\rho)e^{-h\varpi}\},$$

and
$$R = (c^2\xi^2-g\varpi)\exp\{(h-f)\varpi\}-(c^2\xi^2+g\varpi)\exp\{-(h-f)\varpi\}.$$

When expressed in polar co-ordinates, which are defined by

$$\xi = \varpi\cos\theta, \quad \zeta = \varpi\sin\theta, \tag{21}$$

equation (19) becomes

$$\phi_0 = \frac{m}{r_1}+\frac{m}{\pi c^2}\int_0^{\frac{1}{2}\pi}d\theta\int_0^{\infty}\frac{M(\theta,\varpi)\cos(\varpi x\cos\theta)\cos(\varpi z\sin\theta)}{(\varpi-\varpi_0)g(\theta,\varpi)}\,d\varpi, \tag{22}$$

where

$$M(\theta,\varpi) = \sec^2\theta\{(c^2\varpi\cos^2\theta+g)$$
$$\times[-(\rho'+\rho)c^2\varpi\cos^2\theta+(\rho'-\rho)g]\exp\{-(h-f-y)\varpi\}$$
$$-(\rho'-\rho)(c^2\varpi\cos^2\theta-g)(c^2\varpi\cos^2\theta+g)\exp\{-(h+f-y)\varpi\}$$
$$+(\rho'-\rho)(c^2\varpi\cos^2\theta-g)^2\exp\{(h-f-y)\varpi\}$$
$$-(\rho'-\rho)(c^2\varpi\cos^2\theta+g)(c^2\varpi\cos^2\theta-g)\exp\{-(h-f+y)\varpi\}, \tag{23}$$

$$\varpi_0 = gc^{-2}\sec^2\theta, \tag{24}$$

$$g(\theta,\varpi) = \cos^2\theta(\varpi\rho'c^2\cosh h\varpi+\varpi\rho c^2\sinh h\varpi)-(\rho'-\rho)g\sinh h\varpi. \tag{25}$$

To check the condition (10), it will be necessary to find the limit of this integral as $x\to\infty$. To do this, first note that the singularities of the integrand lie on two

curves, $\varpi = \varpi_0$, where ϖ_0 is given by (24) and $\varpi = \varpi_1$, where ϖ_1 is given by the implicit relation

$$g(\theta, \varpi_1) = 0. \tag{26}$$

The curves do not intersect. They are shown roughly in figure 1. The second of these curves behaves in a manner dependent on F, the ratio of the speed to the critical internal wave speed, i.e.

$$F^2 = c^2\rho'/\Delta\rho gh, \quad \Delta\rho = \rho' - \rho. \tag{27}$$

Now consider the integration with respect to ϖ for a fixed value of θ and for large x. It is clear that the interval of integration can be broken into two parts: I_1 from 0 to ϖ_2 and I_0 from ϖ_2 to ∞, where $\varpi_0 > \varpi_2 > \varpi_1$.

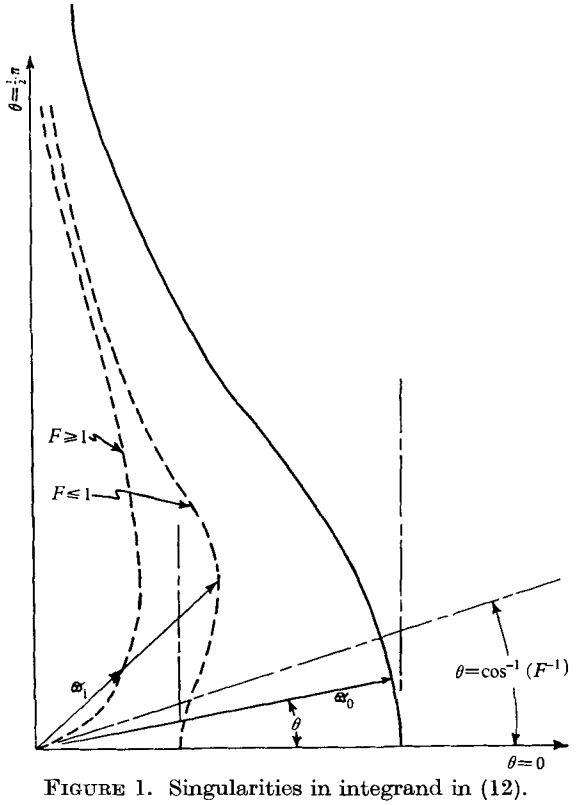

FIGURE 1. Singularities in integrand in (12).

The limit of the integral over each interval as x goes to ∞ may now be evaluated† by means of the Fourier single-integral limit theorem

$$\lim_{t\to\infty}\int_a^b f(s)\frac{\sin[t(s-s_0)]}{s-s_0}\,ds = \begin{cases} \frac{1}{2}\pi[f(s_0+0)+f(s_0-0)] & (a < s_0 < b), \\ \frac{1}{2}\pi f(a+0) & (a = s_0), \\ \frac{1}{2}\pi f(b-0) & (b = s_0), \\ 0, \quad a > s_0 \quad \text{or} \quad b < s_0. \end{cases} \tag{28}$$

The limit is zero in each case if the cosine function occurs instead of the sine function in (28).

† The application of this theorem to the question of the condition at infinity in ship wave problems is due to John V. Wehausen.

For the interval that includes the singularity at ϖ_0, only the first term in $M(\theta, \varpi)$ gives a non-zero contribution. That term can readily be written in a form such that the foregoing theorem applies. This part of the integral then gives

$$\lim_{x\to\infty} I_0 = \frac{4m\rho g}{c^2}\int_0^{\frac{1}{2}\pi} \frac{\exp\{-(h-f-y)\varpi_0\}\sec^2\theta\sin(xg\sec\theta/c^2)\cos(zg\sin\theta\cos^2\theta/c^2)\,d\theta}{\rho\exp(h\varpi_0)+(\rho'-\rho)\exp(-h\varpi_0)}. \tag{29}$$

Since this term is not zero, ϕ_0 as given by (22) violates the condition at $x = +\infty$. This can be rectified by subtracting this expression from (22). It is clear that this expression satisfies Laplace's equation; together with the other parts of the solution, it satisfies the boundary conditions.

The integral over the interval that includes the singularity at ϖ_1 can also be put into a form such that the theorem applies, although the fact that ϖ_1 is given only implicitly by $g(\theta, \varpi_1)$ requires special treatment. This part of the integral then gives

$$\lim_{x\to\infty} I_1 = -\frac{m}{c^2}\int_a^{\frac{1}{2}\pi} \frac{M(\theta,\varpi)\sin(x\varpi_1\cos\theta)\cos(z\varpi_1\sin\theta)\,d\theta}{(\varpi_1-\varpi_0)\,G(\theta,\varpi_1)}, \tag{30}$$

where $a = \cos^{-1}(F^{-1}), \quad F \geqslant 1; \quad a = 0, \quad F < 1,$

$$\begin{aligned} G(\theta,\varpi_1) = {} & \rho' c^2\cos^2\theta\cosh h\varpi_1 + h\rho'\varpi_1 c^2\cos^2\theta\sinh h\varpi_1 \\ & + h\varpi_1\rho c^2\cos^2\theta\cosh h\varpi_1 + \rho c^2\cos^2\theta\sinh h\varpi_1 \\ & - h(\rho'-\rho)\,g\cosh\varpi_1. \end{aligned}$$

Since this term is not zero, it too is subtracted from (22). Thus the total expression for the velocity potential in the layer,

$$\phi = \phi_0 - \lim_{x\to\infty} I_0 - \lim_{x\to\infty} I_1,$$

is obtained from (22), (29), and (30).

3. Forces on a thin ship

Consider a 'thin' ship in steady motion having a speed c in the direction of the x-axis, the co-ordinate system being the same as that used previously. For a deep ocean, the linearized equations have been used† to demonstrate that the ship may be replaced effectively by a distribution of sources over the centreplane section whose strength is given by $-\frac{1}{2}c\pi^{-1}\zeta_\alpha(\alpha,\beta)$, where the shape of the hull is given by $\zeta(x, y)$. This leads to a velocity potential

$$\Phi(x,y,z) = \iint_{S_0} -\tfrac{1}{2}c\pi^{-1}\zeta_\alpha(\alpha,\beta)\,H(x,y,z;\,\alpha,\beta,0)\,d\alpha\,d\beta, \tag{31}$$

where S_0 is the area of the centreplane section, and H is the potential for a 'Havelock source'. The resistance, R, to the motion of the ship is then given by

$$R = 2\rho c\iint_{S_0} \Phi_x(x,y,0)\,\zeta_x(x,y)\,dx\,dy, \tag{32}$$

where, it turns out, some of the terms in Φ_x make no contribution.

† See Lunde (1951).

The same procedure may be applied to the case of a thin ship in a two-layer ocean. Again, the ship may be replaced effectively by a distribution of sources over the centreplane section whose strength is given by $-\frac{1}{2}c\pi^{-1}\zeta_\alpha(\alpha,\beta)$, where the shape of the hull is given by $\zeta(x,y)$. The velocity potential is

$$\Phi(x,y,z) = \iint_{S_0} -\tfrac{1}{2}c\pi^{-1}\zeta_\alpha(\alpha,\beta)\,\phi(x,y,z;\alpha,\beta,0)\,d\alpha\,d\beta, \tag{33}$$

where $\phi(x,y,z;\alpha,\beta,0)$ is given by (22) minus (29) and (30), with the following modification. The source had been taken at $(0,f,0)$. We now replace f by β and x by $(x-\alpha)$. The resistance to the motion of the ship is given by substituting this into (32).

The contribution to R from the x-derivative of the part of ϕ given by (22) is zero. Thus

$$\begin{aligned} R = \frac{4\rho^2 g^2}{\pi c^2}\iint_{S_0} dx\,dy\,\zeta_x(x,y)\iint_{S_0} d\alpha\,d\beta\,\zeta_\alpha(\alpha,\beta) \\ \times\int_0^{\frac{1}{2}\pi}\frac{\exp\{-(h-\beta-y)\,\varpi_0\}\sec^3\theta\cos\{g(x-\alpha)\sec\theta/c^2\}}{\rho\exp(h\varpi_0)+(\rho'-\rho)\exp(-h\varpi_0)}\,d\theta \\ -\frac{\rho}{\pi}\iint_{S_0} dx\,dy\,\zeta_x(x,y)\iint_{S_0} d\alpha\,d\beta\,\zeta_\alpha(\alpha,\beta) \\ \times\int_a^{\frac{1}{2}\pi}\frac{\varpi_1\cos\theta\,M(\theta,\varpi_1)\cos[(x-\alpha)\,\varpi_1\cos\theta]}{(\varpi_1-\varpi_0)\,G(\theta,\varpi_1)}\,d\theta. \end{aligned} \tag{34}$$

If h is made infinitely great, the second term goes to zero, and the first term goes over into the well-known Michell's integral for the wave-making resistance of thin ships

$$\begin{aligned} R = \frac{4g^2\rho}{\pi c^2}\iint_{S_0} dx\,dy\,\zeta_x(x,y)\iint_{S_0} d\alpha\,d\beta\,\zeta_\alpha(\alpha,\beta)\int_0^{\frac{1}{2}\pi} d\theta\sec^3\theta \\ \times\exp\{g(y+\beta)\sec^2\theta/c^2\}\cos\{g(x-\alpha)\sec\theta/c^2\}, \end{aligned} \tag{35}$$

where here the origin lies in the undisturbed free surface. Thus (34) is a generalization of Michell's integral to the case of the two-layer ocean.

4. The asymptotic evaluation of the velocity potential of the ship's internal wave system

The results given above for the velocity potential due to a moving simple source are so complex that a general evaluation of the integrals does not appear to be possible. However, an asymptotic solution for large negative values of x would be useful in delineating the wave pattern far aft of the moving source.

The double integral in (22) is first reduced (asymptotically) to a single integral. The method used is exactly the same as that used to obtain (29) and (30). Note, however, that large negative values of the parameter, x, are considered. This changes the sign of the limits given by (29) and (30) and further leaves error terms of Ox^{-1}. Thus, to this degree of approximation, for $x < 0$,

$$\begin{aligned} \phi(x) \sim \frac{-8\rho g m}{c^2}\int_0^{\frac{1}{2}\pi}\frac{\exp\{-(h-f-y)\,\varpi_0\}}{\rho\exp(h\varpi_0)+(\rho'-\rho)\exp(-h\varpi_0)}\sec^2\theta\sin(gx\sec\theta/c^2) \\ \times\cos(gz\sec^2\theta\sin\theta/c^2)\,d\theta \\ +\frac{2m}{c}\int_a^{\frac{1}{2}\pi}\frac{M(\theta,\varpi_1)\sin(x\varpi_1\cos\theta)\cos(z\varpi_1\sin\theta)}{(\varpi_1-\varpi_0)\,G(\theta,\varpi_1)}\,d\theta. \end{aligned} \tag{36}$$

The first integral has been evaluated for $z = 0$ (i.e. on the track) by the method of steepest descent, but the details will not be presented here. The result of the evaluation showed that the wavelength on the axis was exactly the same as that for a homogeneous ocean, and that the amplitude was only slightly different. The first integral will not be considered further here.

The second integral term in (36) describes the internal wave mode for large negative values of x. The asymptotic evaluation is difficult because ϖ_1 is not given as an explicit function of θ; there is only the implicit relation (26). Simplification is achieved if (26) is used to transform the integral so that the variable of integration is ϖ. It helps further if polar co-ordinates are used for the point of observation, i.e.

$$x = R\cos\gamma, \quad z = R\sin\gamma. \tag{37}$$

The second integral in (36), (call it I_2), has the form

$$I_2(R,\gamma) = \operatorname{Im}\int_b^\infty g(\varpi)\left[\exp\{iRh_+(\varpi)\} + \exp\{iRh_-(\varpi)\}\right]d\varpi, \tag{38}$$

where $b = 0$, $F \geqslant 1$; $b = \varpi_1(0)$, $F < 1$, and where $g(\varpi)$ is continuous and the $h(\varpi)$'s have non-zero second derivatives almost everywhere in the interval of integration, and $\varpi_1(0)$ is obtained from (26) with $\cos\theta$ set equal to unity.

It is well known that the major part of the value of the integrals in (38) arises from the vicinity of the end-points and from the vicinity of those ϖ at which $h(\varpi)$ is stationary, i.e. $h'(\varpi) = 0$; the first-order approximation of the contribution of the stationary points, being of $O(R^{-\frac{1}{2}})$, is more important than the contribution from the end-points which are of $O(R^{-1})$. If there is a stationary point, the first approximation is

$$\begin{aligned} I_2(R,\gamma) \sim{}& \operatorname{Im}\left[2\pi/Rh''_+(\varpi_2)\right]^{\frac{1}{2}} g(\varpi_2)\exp\{i[Rh_+(\varpi_2)+\tfrac{1}{4}\pi]\} \\ &+ \operatorname{Im}\left[2\pi/Rh''_-(\varpi_3)\right]^{\frac{1}{2}} g(\varpi_3)\exp\{i[Rh_-(\varpi_3)+\tfrac{1}{4}\pi]\}; \end{aligned} \tag{39}$$

here ϖ_2, ϖ_3, are the stationary points. The stationary points are given by the solutions of

$$\left.\begin{aligned} \mp\tan\gamma &= \frac{A\sinh Z + Z}{2F^2ZA^2 - A\sinh Z - Z}\left(\frac{F^2ZA - \sinh Z}{\sinh Z}\right)^{\frac{1}{2}}, \\ A &= \cosh Z + (\rho/\rho')\sinh Z \quad (Z = h\varpi). \end{aligned}\right\} \tag{40}$$

The right side of (40) is real and non-negative for all values of Z in the interval of integration. Hence, for all Z there is a γ for which (40) is satisfied. For h_+, the upper sign is used and γ is the second quadrant; for h_-, the lower sign is used and γ is in the third quadrant. The two γ's are symmetrical about π, and the two terms in (39) are equal for these values of γ. Thus only one of the terms in (39) need be computed; let it be the first.

The solution of (40) is plotted in figure 2 for $F = \frac{1}{2}$. The value of γ is π at the lower limit of the range of Z. As Z increases, γ decreases to a minimum, then increases and becomes asymptotic to π as $Z \to \infty$. The minimum point on the curve defines a critical angle, $\gamma_c = 2{\cdot}7933$. For γ smaller than γ_c, there is no solution, and hence no stationary point. Thus for $\gamma_c > \gamma$, ϕ is $O(R^{-1})$. For $\gamma_c < \gamma \leqslant \pi$, there are two solutions to (40), and hence two contributions to ϕ

of the form (39). These represent waves (as will be emphasized later), and hence there are two sets of waves for this case. This picture is true for quite a range of F for which calculations have been made, (see figure 4 for γ_c as a function of F), and is probably true for all $F < 1$.

The solution of (40) is plotted in figure 3 for $F = 2$. The value of γ_c is 2·618 for $Z = 0$, increases monotonically with increase in Z, and it becomes asymptotic to π for large values of Z. Thus for $\gamma < \gamma_c$, ϕ is $O(R^{-1})$ while within the sector ϕ is $O(R^{-\frac{1}{2}})$. Note that for $\gamma_c \leqslant \gamma \leqslant \pi$ there is only one stationary point and, hence,

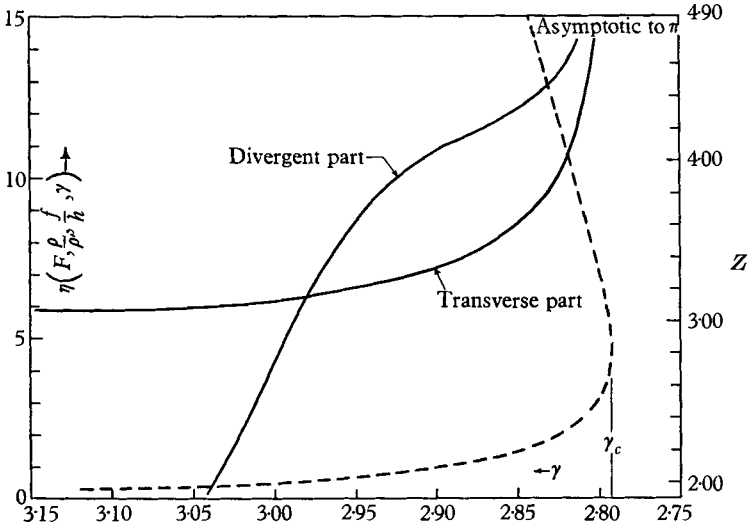

FIGURE 2. Stationary points, Z, and non-dimensional displacement factor η *vs* γ for $F = \frac{1}{2}$, $\rho/\rho' = 0{\cdot}999$, $f/h = 0{\cdot}1$. — Non-dimensional displacement factor, $\eta(F, \rho/\rho', f/h, \gamma)$. – – – Stationary points Z.

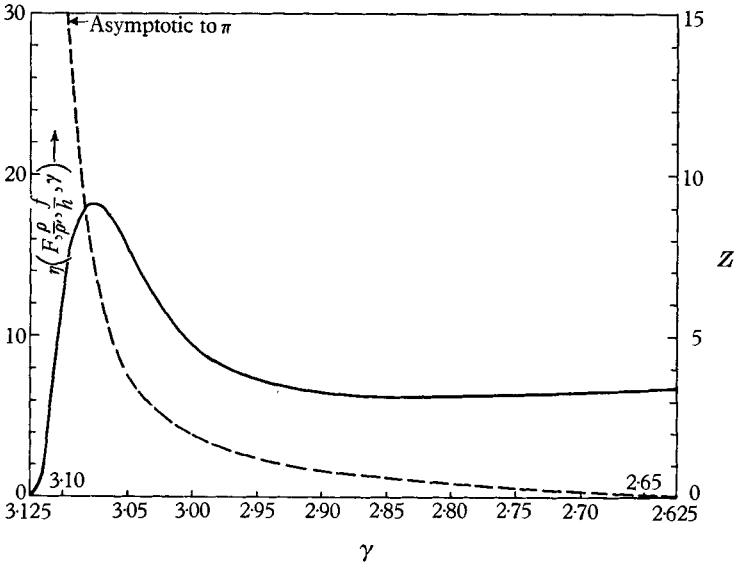

FIGURE 3. As for figure 2, but with $F = 2$.

only one set of waves propagates. This also has been verified for a wide range of values of $F > 1$. A remarkably simple expression can be obtained from (40) for γ_c when $F > 1$,

$$\pi - \gamma_c = \sin^{-1}(F^{-1}). \tag{41}$$

This is just the Mach shock angle formula! This is also plotted in figure 4.

Let the symbol Z now stand for a stationary value of Z. The first approximation of the contribution of a stationary point to the velocity potential of the internal wave is

$$\begin{aligned} I_2(R,\gamma) \sim \operatorname{Im} m &\left[\frac{\pi F A^{\frac{3}{2}}}{Rh}\right]^{\frac{1}{2}} \\ &\times \left\{ \frac{\cos\gamma}{Z\sin Z}\left[2A\cosh Z\,(Z\sinh Z)^{\frac{1}{2}} - (A\sinh Z + Z)\frac{(\sinh Z + Z\cosh Z)}{2(Z\sinh Z)^{\frac{1}{2}}}\right]\right. \\ &+ \frac{\sin\gamma}{F^2Z^2A - Z\sinh Z}\left[(F^2Z^2A - Z\sinh Z)^{\frac{1}{2}}\,(2F^2A^2 + 4F^2ZAB - 2A\cosh Z)\right. \\ &\left.\left. - (2F^2Z^2A^2 - A\sinh Z - Z)\frac{(2F^2ZA + F^2Z^2B - \sinh Z - Z\cosh Z)}{2(F^2Z^2A - Z\sinh Z)^{\frac{1}{2}}}\right]\right\}^{-\frac{1}{2}} \\ &\times \left\{ -(\rho C + \rho' D)\,C\exp\left[-\left(1 - \frac{f}{h} - \frac{y}{h}\right)Z\right] - (\rho' - \rho)\,CD\exp\left[-\left(1 - \frac{f}{h} + \frac{y}{h}\right)Z\right]\right. \\ &\left. + (\rho' - \rho)\,D^2\exp\left[\left(1 - \frac{f}{h} - \frac{y}{h}\right)Z\right] - (\rho' - \rho)\,CD\exp\left[-\left(1 - \frac{f}{h} + \frac{y}{h}\right)Z\right]\right\} \\ &\times [D\cos\theta\sin\theta\rho' c^2 ZA]^{-1}\exp\{i[RZ\cos(\theta - \gamma)/h + \tfrac{1}{4}\pi]\}, \end{aligned} \tag{42}$$

where

$$B = \sinh Z + \frac{\rho}{\rho'}\cosh Z, \quad C = \frac{c^2\sinh Z}{F^2A} + gh, \quad D = \frac{c^2\sinh Z}{F^2A} - gh.$$

Here the angle θ is computed from (26), with Z taken at the stationary point. For $F < 1$, there would be two such terms, one for each stationary point at a given γ; for $F > 1$, there would be only one term.

5. The evaluation of the displacement of the interface

We recall a relation at the interface

$$\phi_y(x, 0, z) = -c\eta_x. \tag{43}$$

The expression for η, the displacement of the interface† can readily be obtained for values of γ restricted to $\gamma_c \leqslant \gamma \leqslant \pi$. The solutions can be written in the form

$$\eta = \frac{1}{c}\frac{m}{R^{\frac{1}{2}}h^{\frac{1}{2}}}\eta\left(F, \frac{\rho}{\rho'}, \frac{f}{h}, Z\right)\begin{matrix}\cos\\ \sin\end{matrix}[RZ\cos(\theta - Z)/h + \tfrac{1}{4}\pi], \tag{44}$$

† The displacement of the interface due to the surface mode will not be considered. Thus, only the first-order contribution to the velocity potential from the stationary points in I_2 as given by (42) is used.

where

$$\eta\left(F,\frac{\rho}{\rho'},\frac{f}{h},Z\right) = (\pi FA)^{\frac{1}{2}}(ZA\sin\theta\cos^2\theta)^{-1}$$

$$\times\left\{\frac{\cos\alpha}{Z\sinh Z}\left[2A\cosh Z(Z\sinh Z)^{\frac{1}{2}} - (A\sinh Z+Z)\frac{\sinh Z+Z\cosh Z}{2(Z\sinh Z)^{\frac{1}{2}}}\right]\right.$$

$$+\frac{\sin\alpha}{F^2Z^2A-Z\sinh A}\left[(F^2Z^2A-Z\sinh Z)^{\frac{1}{2}}(2F^2A^2+4F^2ZBA-2A\cosh Z)\right.$$

$$\left.\left.-(2F^2ZA^2-A\sinh Z-Z)\frac{(2F^2ZA-F^2Z^2B-\sinh Z-Z\cosh Z)}{2(F^2Z^2A-Z\sinh Z)^{\frac{1}{2}}}\right]\right\}^{-\frac{1}{2}}$$

$$\times\left\{-\frac{C}{D}\frac{(\rho C+\rho' D)}{\rho' c^2}\exp\left\{-\left(1-\frac{f}{h}\right)Z\right\}-\frac{\Delta\rho}{\rho' c^2}D\right.$$

$$\left.\times\exp\left\{\left(1-\frac{f}{h}\right)Z\right\}+\frac{2\Delta\rho}{\rho' c^2}C\exp(-Z)\sinh Z\right\}$$

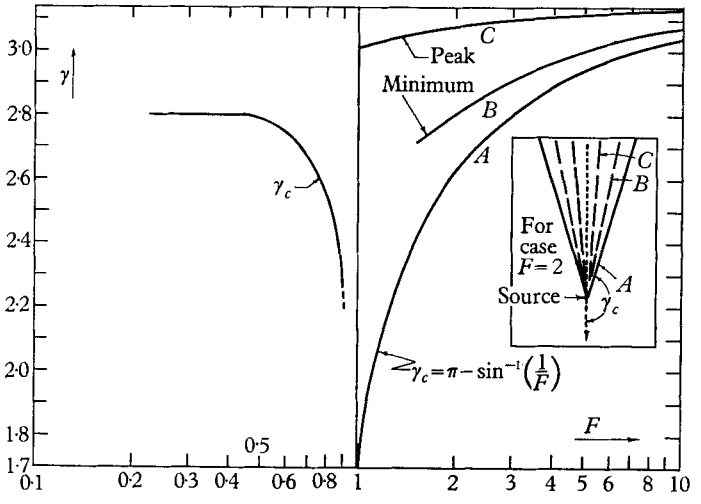

FIGURE 4. Features of $\eta(F, \rho/\rho', f/h, \gamma)$ *vs* F. Curve A gives the value of γ_c, curve B the value of γ for which η is a minimum, and curve C that for which η is a maximum.

is a non-dimensional displacement factor which is a function of the non-dimensional parameters F, ρ/ρ', f/h and the variable Z. This non-dimensional displacement factor has been computed and is plotted *vs* Z in figures 2 and 3 for $F = \frac{1}{2}$ and $F = 2$, with $\rho/\rho' = 0{\cdot}999$ and $f/h = 0{\cdot}1$. On the same graphs is plotted γ *vs* Z for the stationary values of Z.

Note that $\eta(\frac{1}{2}, \rho/\rho', f/h, Z)$ has a singularity at γ_c because $h''(\gamma_c)$ is zero. For $F = 2$, $\eta(F, \rho/\rho', f/h, Z)$ is well behaved for all Z. Here, there is a maximum at $\gamma = 3{\cdot}075$ and a minimum at $\gamma = 2{\cdot}807$.

Computations for a wide range of ratios of speed to the critical internal wave speed, i.e. F, are summarized in figures 4 and 5. In figure 4 the critical angle is plotted as a function of F for a range of $F < 1$, and for $1 \leqslant F \leqslant 10$. Note that as

F increases from a small value to unity, the half-angle of the wedge, $\pi-\gamma_c$, within which the sensible waves are contained, increases; at $F = 1$, it is $\frac{1}{2}\pi$, and for $F > 1$ it obeys the law: $\pi-\gamma_c = \sin^{-1}(F^{-1})$. Also plotted in this figure are the positions of the maxima and the minima of the non-dimensional amplitude as functions of F. In figure 5, the amplitudes of the non-dimensional amplitude at the maxima, minima, and boundary points are plotted as functions

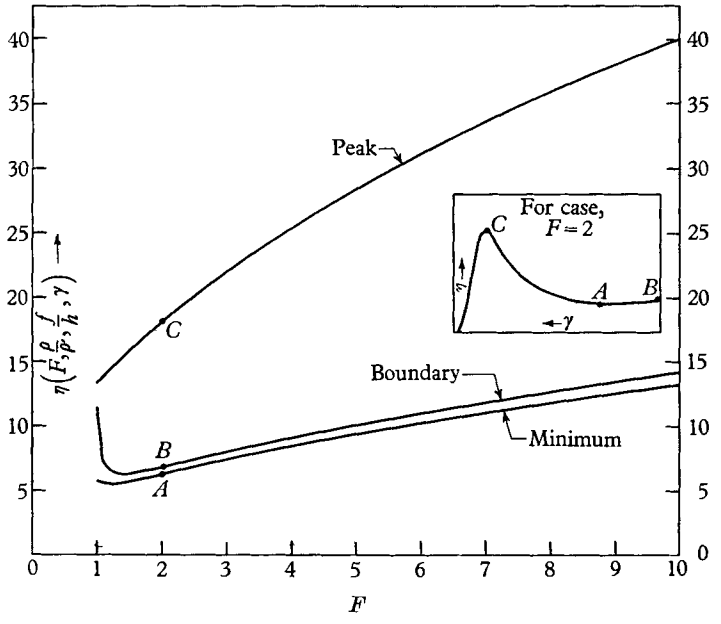

FIGURE 5. Amplitudes of maxima, minima and boundary points of $\eta(F, \rho/\rho', f/h, \gamma)$ *vs* F.

of F. Note the increase with F, which is surprising in view of the commonly held notion that the 'dead water' effect is greatly decreased for F even a small amount larger than unity.

Consider the argument of the oscillatory factor in (44). It can be written

$$RZ\cos(\theta-\gamma)/h+\tfrac{1}{4}\pi = 2\pi R/\lambda(Z)+\tfrac{1}{4}\pi, \tag{45}$$

from which it is clear that the displacement, η, along a ray, γ = constant, is wavelike. If there are two stationary values of Z for a given γ, there are two terms in (44), and hence two λ's. Thus for $F < 1$, there are two wave systems. This can be brought out further by delineating the position of the crests. This is done by setting

$$RZ\cos(\theta-\gamma)/h+\tfrac{1}{4}\pi = 2\pi N \quad \text{or} \quad 2\pi N+\tfrac{1}{2}\pi, \tag{46a,b}$$

for the cosine case and the sine case respectively, in (44), and where N is an integer. Here, Z is the stationary value for the given γ, and θ is a function of Z as previously given. Computations have been made using (26) and (40) in (46) for the same set of parameters as in figures 2 and 3. The results for $F = \frac{1}{2}$ are shown in figure 6 for four values of N. That there are two sets of waves is clear; they are

quite similar to the sets of transverse waves and divergent waves caused by a ship in an infinitely deep, homogeneous ocean. The wavelength of the transverse wave on the track is such that a plane wave having that wavelength travels at one half the critical internal wave speed. But this is just the assumed speed of the simple source. Note that the crests of the two different waves do not meet at the edge of the wedge. There is a singularity in the displacement due to the breakdown in the usual first term in the expansion by the method of stationary

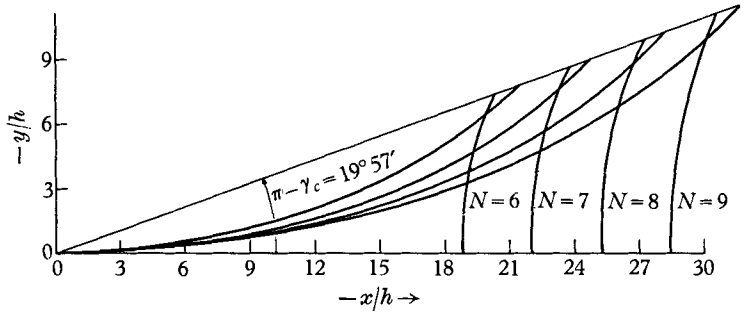

FIGURE 6. Internal wave crests for $F = \frac{1}{2}$, $\rho/\rho' = 0{\cdot}999$, $f/h = 0{\cdot}1$.

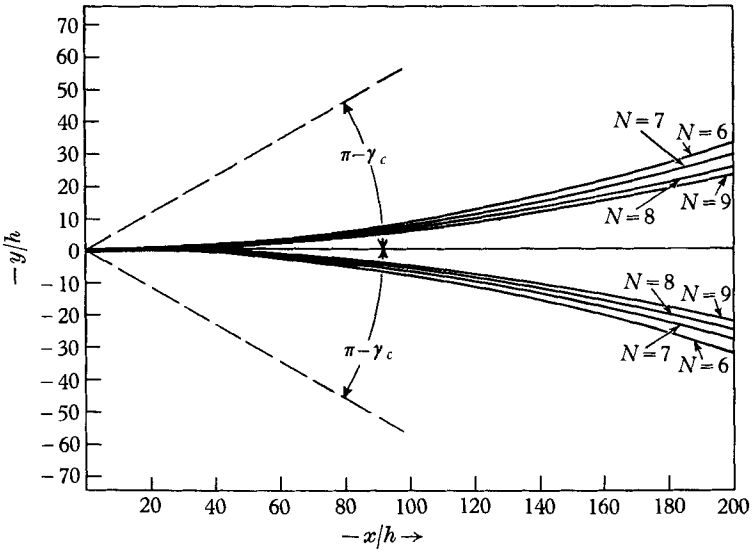

FIGURE 7. Internal wave crests for $F = 2$, $\rho/\rho' = 0{\cdot}999$, $f/h = 0{\cdot}1$.

phase. A modification of the computation in the vicinity of this point (it would be almost intractable) would probably show a gradual transition in the wave front here. The results for $F = 2$ are shown in figure 7. Here there is only one set of waves, the divergent waves.

From (44) it is clear that the displacement for any point of the crest is proportional to the product of the factors $R^{-\frac{1}{2}}$ and $\eta(F, \rho/\rho', f/h, Z)$. To visualize the amplitude of the crest, an interval, proportional to this product, perpendicular to the curve of the crest at each point on the crest is drawn, and the end-points

are connected. In figure 8 this is done for a single crest ($N = 6$) for $F = \frac{1}{2}$, and in figure 9 this is done for a single crest ($N = 6$) for $F = 2$. In each case, a three-dimensional sketch is also given to give a clearer picture of the amplitude of the crest.

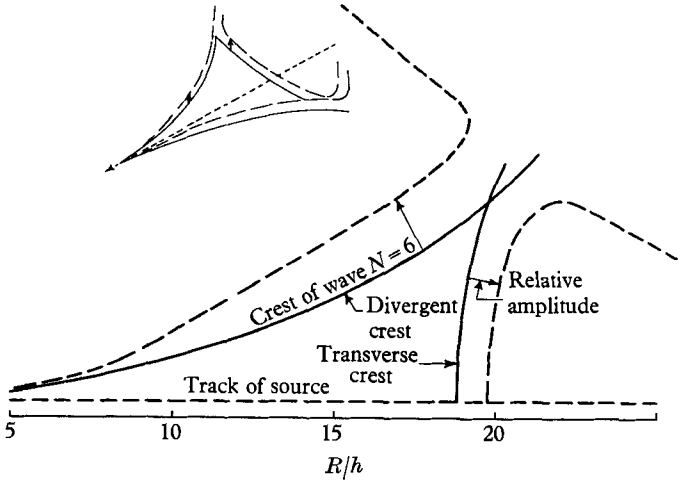

FIGURE 8. Height of internal wave crest for $F = \frac{1}{2}$, $\rho/\rho' = 0{\cdot}999$, $f/h = 0{\cdot}1$.

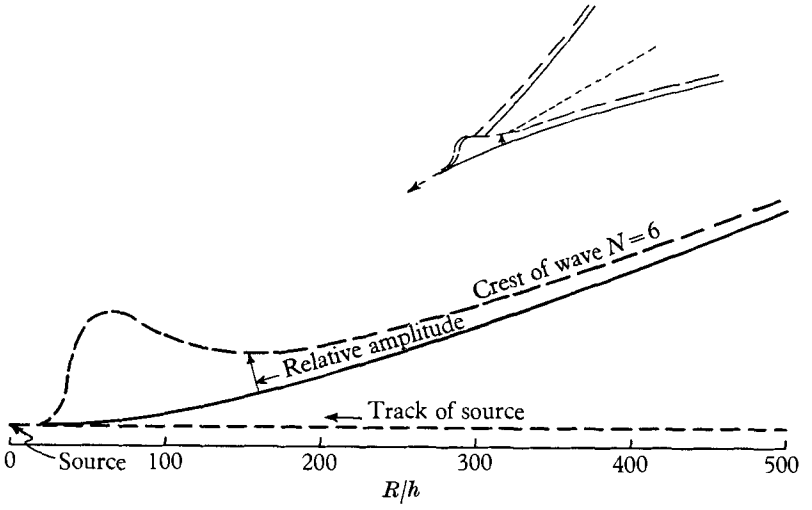

FIGURE 9. Height of internal wave crest for $F = 2$, $\rho/\rho' = 0{\cdot}999$, $f/h = 0{\cdot}1$.

6. Discussion

An integral formula for the wave-making resistance has been developed. It would be worthwhile to use this result to show how the resistance varies with speed. In particular, it would be of interest to see if there is a sudden decrease in resistance with speed at the critical internal wave velocity.

The displacement of the interface due to the internal wave mode has been described in some detail. It would also be worthwhile to treat in detail the surface wave mode to see what effect the stratification of the water has on it.

The author wishes to acknowledge the many helpful suggestions given by Professor John V. Wehausen of the University of California, Berkeley. He is also indebted to Robert Arenz for programming and executing many of the computations, and to David Brumley and the NEL drafting staff for assistance with the figures.

REFERENCES

EKMAN, V. W. 1904 On dead water. Norwegian North Polar Expedition, 1893–1896. *Sci. Res.* **5**, Christiana.

HOGNER, E. 1923 Contributions to the theory of ship waves. *Arch. Mat. Astr. Fys.* **17**, 1–50.

HUDIMAC, A. A. 1958 The motion of a body in a fluid with a free surface and irregular solid boundaries. Dissertation Univ. Calif. May 1958; also *Univ. Calif. Inst. Engng Res.* Berkeley, Calif. Ser. **85**, no. 5.

KELVIN, LORD, 1887 On the waves produced by a single impulse in water of any depth, or in a dispersive medium. *Proc. Roy. Soc.* A, **42**, 80–5.

KOCHIN, N. E. 1949 *Collected Works* (Academy of Sciences USSR), Vol. I, pp. 448, 508.

LAMB, H. 1916 On waves due to a travelling disturbance, with an application to waves in superposed fluids. *Phil. Mag.* **31**, 386–99.

LUNDE, J. K. 1951. On the linearized theory of wave resistance of displacement ships in steady and accelerated motion. *SNAME*, **59**, 26–76.

PETERS, A. S. 1949 A new treatment of the ship wave problem. *Commun. Pure Appl. Math.* **2**, 123–48.

SRETENSKII, L. N. 1959 On the wave resistance of ships in the presence of internal waves. *Izv. Akad. Nauk C.C.C.R., Otdelenie Tekhnicheskikh*, **1**, 56–63.

TIMMAN, R. & VOSSERS, G. 1953 The linearized velocity potential round a Michell-ship. *Technische Hogeschool, Laboratoriam voor Scheepsbouwkaunde, Delft, Rappart* **1**,

WARREN, F. W. G. 1960 Wave resistance to vertical motion in a stratified fluid. *J. Fluid Mech.* **7**, 209–29.